AN IMAGE PRE-PROCESSING AND CLASSIFICATION APPLICATION AND THE EXPERIMENTATION ANALYSIS OF THE AGRICULTURE CHANGE DETECTION FOR THE DIFFERENT LULC CLASSES USING REMOTE SENSING TIME SERIES IMAGES.

Mr. Hareesh B[1*], Mr. Vasudeva[2]

Abstract:
Detecting changes in land use and land cover (LULC) using remote sensing data is an essential source of information for many decision support systems like land conservation, sustainable development, water resource management, etc. All these systems are well resourced with the help of extracted and analysed data produced from land use and land cover change detection. This study aims to determine land use and land cover changes in the western Ghat basins. The proposed study is to find the change in agriculture patterns over the years using various segmentation and LULC classification techniques. The remote sensing data which is to be used for the classification required to be pre-processed. The study elaborates the analysis of different image pre-processing, segmentation and classification algorithms to analyse the dominance of the commercial plantation crops over the food-related crop culture.

Keywords: Remote sensing, Image Pre-processing, Segmentation, Classification

[1*]Associate Professor, Department of Computer Applications, St. Joseph Engineering College, Vamanjoor, Mangaluru
[2]Professor, Nitte (Deemed to be University), NMAM Institute of Technology, Department of Information Science and Engineering, Nitte, India

***Corresponding Author:** Mr. Hareesh B
*Associate Professor, Department of Computer Applications, St. Joseph Engineering College, Vamanjoor, Mangaluru

DOI: 10.48047/ecb/2023.12.si10.0039

1 INTRODUCTION

1.1 Background of the work

The change in land use on agricultural land can be precisely measured using remote sensing techniques. High-resolution remote sensing images may be processed to assess different land use categories utilizing powerful image processing tools and algorithms following recent advancements in remote sensing applications.

Remote sensing (RS) can be characterized in a variety of ways, but in its most basic form, as well as with current advancements in the area, it can be described as a process of acquiring images for various processing approaches employing high-definition onboard sensors [1]. The electromagnetic energy acquired by these sensors is in the form of reflected energies from the earth at various wavelengths (EM). These energy properties are also influenced by the object's radiation, temperature, and emissivity. The recorded remote sensing image is measured with a mathematical form ranging from 0-255 and is represented in pixels. Objects with different wavelengths follow a pattern in the form of a spectral signature, which indicates the range of values for a class of comparable objects. The correct interpretation of this pattern will lead to the correct identification of the object.

The recent developments in the field of digital imaging have transformed classic digital imaging applications such as algorithmic analysis into more societal activities. Using advances in imaging technologies, competitive and competent remote sensing organizations have made major contributions to this market, despite geographical limits [2]. Object identification from the hyperspectral image is now made simple because of sophisticated imaging algorithms and technologies, especially in the field of LULC. The majority of RS research applications in the past were focused on urban development due to the availability of low-frequency images, but with the availability of various brands of high-frequency images in the last decade, the scope has expanded to include remote villages to plan vegetation, change detection, and thus better crop selection [3].

As a result of new airborne satellites which are providing a global view and often repeating data, LULC change detection can be easily and effectively measured. In the last two decades, globalization and rapid economic growth have resulted in significant land use, which has benefited the country's economy while also causing massive changes in environmental issues such as forest degradation, urbanization, and changes in traditional crop production, to name a few. Each of these negative consequences resulted in a significant shift in global environmental standards. The monitoring of these changes in the aforementioned domain is a critical necessity of this decade to plan, assist, and sustain globally balanced environmental circumstances [4].

The research area is situated between the Western Ghats reservoir in the Subramanya forest area, Sullia Taluk, Dakshina Kannada district of Karnataka, India, and the Arabian Sea in the Mangalore region, which is the epic hotspot of urbanization.

Traditional rice fields in the region were gradually converted to areca nut plantations in the late 1980s and early 1990s. To begin with, the requirement for cash crops has shifted agricultural practices. Second, due to urbanization and changes in economic policies, there are concerns about a skilled labor shortage.

Because of the growth in crop and government policy, the areca nut plantation in this region endured high operational costs, yellow leaf illness, and a massive price drop in the years 2000-10. Farmer's interests changed to rubber plantations and other plantation crops due to good markets and ease of maintenance. The cycle has now been reversed, with the rubber market value plummeting and farmers adjusting their planting patterns yet again. These unique practices resulted in a slew of environmental and societal problems in the area.

As to provide a solution to farmers they do not have access to a proper forecasting system or there is no such accurate and handy system available to know the acres of plantation of various crops or relevant information to cultivate any particular crop. In this thesis, remote sensing applications are used to solve the problem. The graph-theoretical procedures were used to conduct a thorough experimentation review for various algorithmic analyses.

1.2 Agriculture Change Detection Analysis

Detecting changes in land use and land cover (LULC) using remote sensing data is an essential source of information for many decision support systems. Land conservation, sustainable development, and water resource management will benefit from data produced from land use and land cover change detection. The goal of this study is to

determine changes in land use and land cover in the Markanja village of Sullia Taluk of Dakshina District, which is located in the western ghat basin.

Graph-based image processing techniques along with other necessary methodologies were applied to the image data set taken in different intervals to examine the change detection. The 2013 and 2018 Landsat 7, 8, and Google images were used for the experimentation. The software Matlab, QGIS, and IDRISI were used to detect land-use changes [5]. Five land cover classes (water body, bushland, grassland, forestland, cultivated, and residential land) were used for the categorization. The accuracy assessment was tested individually using the kappa coefficient after the preprocessing and segmentation. According to the findings, areca nut and rubber plantations in the basin have expanded by 15.61 percent and 8.05 percent, respectively, over the last 20 years. To preserve the basin from unwanted LULC change, good land management methods, integrated watershed management, and active engagement of the local people should be promoted.

1.3 Data Acquisition Specification

Table 1.1 gives the specification of the image data products being used in this study. The major experimentation process uses Landsat 8 data. For the validation of the classification and to test the older land classes subsequently, Landsat 7,5 and LISS III remote sensing data were used, The verify the created labels and ground truth information in some parts of the study Landsat images were acquired through Google earth pro. The satellite data were procured from the National Remote Sensing Centre (NRSC), Hyderabad, India. The Landsat data are freely acquired from USGS websites. The Google earth pro is used to acquire Google earth images [6].

Table 1.1: Details of the data products used

Sl. No.	Satellite and Data Type	Date of Acquisition	Spectral Bands	Spatial Resolution
1	Landsat 8	16-12-2013	8	30m
2	Landsat 8	10-03-2018	8	30m
3	Google Earth Image	01-02-2013	3	15m
4	Google Earth Image	01-10-2018	3	15m
5	Landsat 7	20-12-2020	6	30m
6	Landsat 5	23-01-1993	6	30m
7	Landsat 5	02-01-1995	6	30m
8	Landsat 5	18-03-2001	6	30m
9	LISS III	23-01-2013	4	24m
10	LISS III	14-01-2018	4	24m

Study Area:

Markanja Village, SulliaTaluk, Dakshina Kannada, Karnataka, India 12.5654° N, 75.5055° E as the test area.

1.4 Problem Statement

In the Dakshina Kannada District of Karnataka, India, land use has been highly exploited lawlessly and extended beyond the mark to a wider extent in various fields, such as agriculture, vegetation, industrialization, and other reasons. This could be due to issues with the economy, government administration, or urbanization. The agricultural field's land use has gradually shifted from conventional paddy farming to areca nut plantations, and now to rubber plantations, pineapple plantations, and other plantations. This gradual adoption of new farming practices leads to a slew of concerns, including an inconvenient wet season, a shift in work culture, labor scarcity, and inconsistencies in commercial issues such as price volatility and other environmental consequences.

There is no information available from any government agency about the amount of which a particular agricultural product or land class is grown in this region. The study helps in analysing the changes in land use structure, as well as their consequences and benefits. By examining the data, proper and effective methodologies can be adopted to address this issue as shown in Figure 1.1.

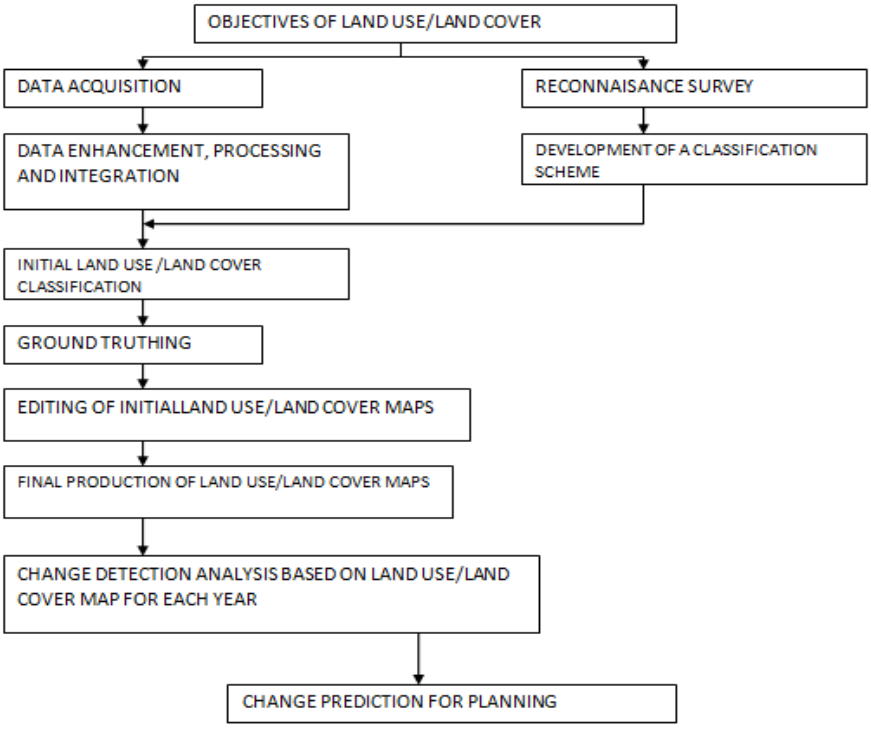

Figure 1.1 Flow of Methodology

2. LITERATURE SURVEY

The spatial interconnections visible in images were not taken into consideration in various image categorization efforts. This chapter intuitively believes that incorporating spatial relations can increase image categorization accuracy. The gSpan graph mining framework for the image as well as a weighting method provides differentiable spatial relations in the image. The common shapes can be used to generate vector features and processed using usual image mining approaches. The efficiency of the weighed system above the non-weighted scheme was the scope for the analysis.

S. S. Sawant and M. Prabukumar [22] elaborated various image segmentation techniques for land use analysis provided extensive knowledge on the different graph-based classification and segmentation approaches. In the beginning, the author abstracted the concept and extent of segmentation and stated that it is the partition of image data into associated relevant pieces or areas. For several image analysis methodologies, segmentation is a crucial step.

The necessity and superiority of the partitioning of the image and its output is a key determinant of how well these image analysis algorithms function. As we know that image data can be partitioned in a variety of techniques, depending on a variety of factors.

Important aspects of the dividing of images for land categorizations are discussed several times in this article. The said aspects objects in the earth which is diverse in its spatial characteristics. The author tries to find different land-use classed. More importantly, the emphasis is on finding the kinds of crops, settlements, etc.

The conclusive remark in the literature for the vegetation classification brings a very important aspect for the study of this thesis. As the primary experimentation for the problem statement experienced that similar vegetation area has different spectral properties. One of the most challenging parts of vegetation mapping is to map the vegetation area with similar vegetation types and similar spectral properties. The author finds it difficult to achieve this by using either classic unsupervised or supervised classification methods.

The whole section is narrated with a wide variety of classification algorithms, each produces differentiable results based on the different context of segmentation. Sometimes the combination of the above said approaches may give better results. The P. Mhangara, W. Mapurisa, and N. Mudau [35] used a hybrid method to map land classes in the metropolitan area of Atlanta with the help of Landsat 7 ETM+ images rendered greater benefits. However, it is to be more cautious while applying

because such a hybrid model was implemented for the specific region and specific data set.

The authors have also given a glimpse of the key technologies that can be used nowadays using advanced imagery and tools to fuse multispectral and multiple band fusion techniques to extract the land cover.

M. Vidal and J. M. Amigo [4] explored the hyper spectral imagery comes with dozens of spectral bands and the sensors used here are better suited for vegetation mapping especially plant species classification as compared to multispectral image classification. Different satellite versions come with different band numbers and the combination of this helps in the evaluation of change detection.

L. Hu, C. Qi, and Q. Wang [17] discussed the highest accuracy was recorded for UAV satellites and the lowest for Pleiades satellites. As already discussed in several articles, the selection of data and algorithms is solely depending on the context of the algorithm and also the ROI. The proposed work uses Landsat imagery because it is available in open source.

The authors reviewed many applications, such as global-scale high-resolution demographic databases, national security, human health, and energy which require accurate identification. To address these issues, this paper proposes a feature that may effectively distinguish between distinct categories.

The important method proposed in this study combines semi and super-pixel tessellation with a semi-supervised classification based on a majorization-minimization strategy that is efficient and non-pipelined. The super pixel representation is a fundamental reason for good categorization. The future work proposed here will focus on extending this approach to temporal data as well as on integrating the feature extraction, selection, and classification into a single scheme to improve the correlation between super pixels and model training.

The Western Ghats in India cover around 1500 Km and fall within the longitude and latitude of 8^0 - 12^0 N from to south from around Tampti to Kanyakumari. It almost covers six states like Gujarath, Maharashtra, Goa, Karnataka, Kerala, Tamilnadu, and few other parts of the union territory.

In its reach, the dense forest spans bio-resources ranging from extremely useful timber–non-timber categories, medicinal plants, food categories, and plantations, among others. As is customary, humans expansionist tendencies substantially triggered land use categories of their own in these areas. The area makes use of the Western Ghats' development of rubber plantations over areca nut plantations.

C Sudhakar Reddy∗, CSJha, and VK Dadhwal [26] deliberate the application of remote sensing in land use analysis of forest land, and the discussion of change of land use goes as follows.

The Western Ghats have a natural forest cover that offers several environmental benefits. Monsoon influence, and hence agriculture activities in the higher and lower belts of the Western Ghat, were significantly connected.

The study illustrates the distortion of forest covers according to the analysis, global forest loss increased by 35% between 1920 and 2013. As this land use classification shows, the most significant change in land use was from forest areas to some agricultural plantations and others. For the change detection of the above type, the authors used the time series temporal data obtained from Landsat-MMS, IRS 1A LISS-1, IRS P6 AWiFS, and Resources at-2 AwiFS satellite.

The article also formulates the compound interest to compute the yearly change in the forest. Six classes and landscape indices were quantified for the change study. FRAGSTATS software is used to calculate the quantization and patch index. The accuracy of the classification is determined by comparing the high-resolution images taken from the Indian remote sensing web portal and Google Earth images obtained from the source site.

T. V. Ramachandra and Setturu Bharath [27] wrote on the critical issue of the Western Ghat region's biodiversity hotspot. The author of this paper highlighted the regional land-use change and its relative disadvantages.

The author here presented CO2 emission statistics in this region and its mitigation in global warming. He also narrated the change o Dagoberto Pulido Dagoberto Pulido f ecosystem in this region. The objective of this article is not part of our problem discussion, even though the paper gives various statistics of the land-use change in this region, which was much helped for our work. The

materials and methodology used here helped to choose the Landsat 8 OLI image data set for the final data analysis, along with the Google earth pro product for the land class verification. The analysis of the land-use change of the study area from 8^0 N to 21^o N latitudes and 73^o E to 77^o E longitudes was experimented by using the following image segmentation steps.

1. Collection of Data from Landsat Satellite
2. ROI Extraction by referring the field verification using Google Earth
3. Data pre-processing is carried out by using 3 steps, at first Geometric corrections are carried out and followed with the radiometric corrections and elevation estimation.
4. False color is generated and stacked over topographic data
5. Developing trained sets
6. Land use classification and accuracy assessment.
7. Modeling and prediction of biomass carbon budgeting
8. Forest Fragmentation analysis

3. Methodology

3.1 Image Fusion

Numerous approaches for merging satellite photos have been proposed in the literature. Image fusion approaches are divided into two categories first one is the transform domain fusion method, where input images were altered using various transformation cubic or linear methods and then fused. The generated fused output should be scaled to the original image state. This process is conducted by applying inverse transformation techniques. The numeric factors for the fusion are yielded with the pixel-based [23].

Another category of fusion approach is by using the spatial feature, where input images are directly processed without transformation as in the transformation domain. Also in this approach, a cost function is used to assess the weights of an input image and its related pixels. The popular list of spatial-based approaches is averaging, broveys, PCA, and HIS.

The alternative spatial fusion approach is the fusion of high-frequency images with up-sampled MS images by using a high pass filtering-based approach. However, the possibility of distortion in the spatial domain may make it difficult to employ in spatially based categories. Furthermore, the detrimental impact of distortion will make the classification procedure more challenging.

This challenging task can be handled using different transform domain techniques such as the Laplacian, curvelet etc. The said techniques along with other algorithms discussed outperform existing spatial fusion approaches in terms of the combined image spatial and spectral effectiveness.

Transform domain techniques to image fusion can handle spatial distortion. Other spatial domain fusion approaches, including Laplacian pyramid procedures, curvelet transformations, and so on, have indeed been proposed. These methods outperform existing spatial fusion approaches in terms of the spatial and spectral efficiency of the fused image.

The fusion approach needs a good collection of image bands in the image repository and needs to be labelled properly. The extracted Landsat 5, 7, 8 band properties are studied with different combinations. The results of band combinations after the fusion are reviewed extensively to avoid any deregistration mistakes in image fusion. The rigorous discussion of image fusion techniques in the literature review section helped to screen out some useful image fusion algorithms, which is discussed in the below section [35].

- IHS transform-based image fusion

The RGB color space organized in the extracted RS images is not sufficient for the possible fusion of different bands since the color channel and its connections are not clearly shown. Separate channels with distinct color attributes, such as intensity (I), hue (H), and saturation (S), can be viewed using IHS (S). The pixel values of RGB are determined by the intensity and two vector values vector 1 and vector 2.

- Brovey Transform (BT)

To sharpen MS images the overall expectation of any fusion technique is used to grid the possible geographical area for future classification assessments. All fusion algorithms mentioned in the literature process the pixel intensities and other characteristics in a variety of processing methods. In brovey method, a ratio P is used to multiply each MS image, and the same is divided by the sum of MS images.

$$Rnew = R\,(R + G + B) \times P\,AN \quad (1)$$
$$Gnew = G\,(R + G + B) \times P\,AN \quad (2)$$
$$Bnew = B\,(R + G + B) \times P\,AN \quad (3)$$

• Wavelet transform image fusion (WT)
The resulting fusion image analysis says that this particular fusion technique exhibits good performance as well as efficiency for different classification applications. The defined fusion rule bundles the images into the transform domain and then transformed them back to the spatial domain with a resultant fused image. The geo-referenced two input images with the coordinate values having I1(x, y) and I2(x, y) are merged with the said rule to conceive the resultant image I(x, y), however, to avoid the distortions the resultant image is reconstructed by using inverse wavelet transform technique w-1.

• Principal component analysis (PCA) based image fusion,
PCA works by mathematically transforming a linear set of, mostly an interconnected value results into a disjoint set of the variable using orthogonal transformations.

The transforming technique causes a data set definition that is both compact and optimal for future processing. As much variation as possible is accounted for by the first principal factor. The path with the greatest variance is assumed to be the first principle variable. The second principal portion must be in an orthogonal subspace to the first variable. The third subspace portion indicates the path of the subspace's largest variance, which is perpendicular to the first two, and so on.

3.2.1 Image Fusion: Results

Since the NIR band is least affected by atmospheric effects, it is used as the high-resolution band in the change detection process. The NIR band is involved in the change detection process causing minute faults in the fusion. The TIR band images are resampled to a resolution of 15 meters per pixel and further merged to construct a particular spectral identity. The importance of the coupling to construct an RGB value for the different bands, which provides a general human interpretable view of the image to the user. Quartz and Sulphate indices are produced by combining OLI bands 2, 3, and 4 into one RGB image and fusing it with a NIR RGB image, while Carbonate and Mafic indices are produced by fusing TIRS bands 10 and 11.

Level 5 of the Wavelet transform decomposition was selected. The mean of both images was chosen as an approximation and data. The Wavelet transform image fusion generated the best results with these settings. Figure 3.1 shows merged images generated with the IHS, Brovey, PCA, and Wavelet transforms.

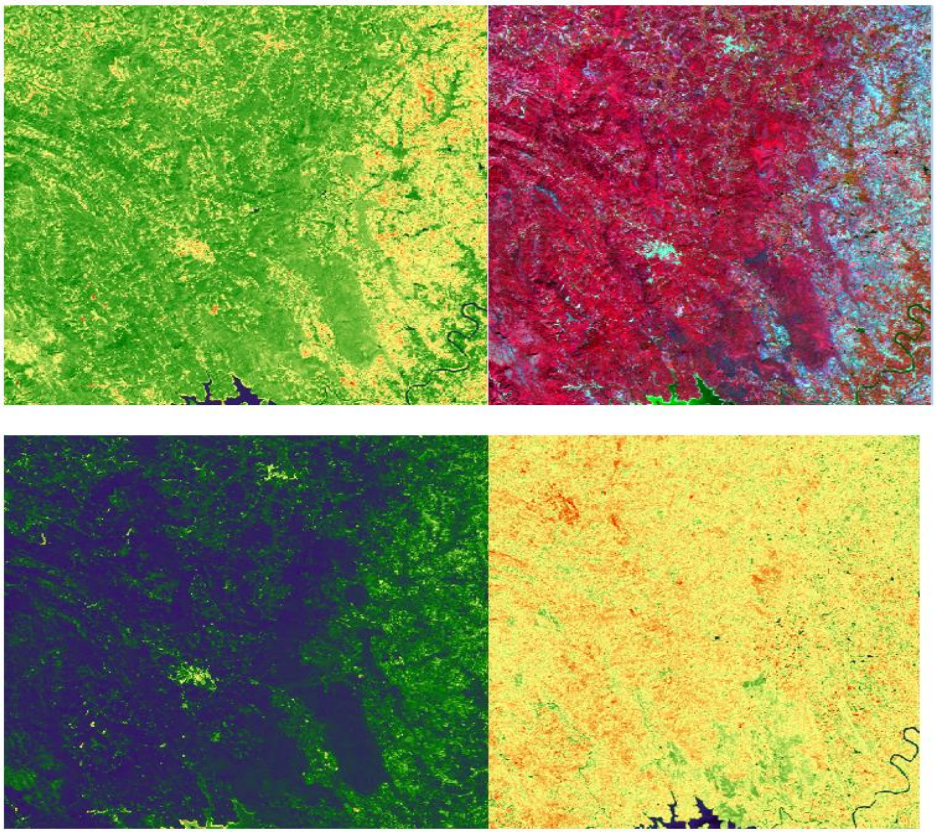

Figure 3.1: Fused images of i) PCA Fusion ii) IHS Fusion iii) Wavelet Transform iv) Brovey Transform

In comparison, the HPCC found that IHS has a substantially higher resolution than the other three approaches when comparing VNIR and fused images for resolution compatibility. As an outcome of this, some 90-meter pixels were divided into smaller 15-meter pixels with distinct DNs., while in the case of the IHS transform, the lack of spectral information dominated the spatial data, resulting in the lower pixels both having the same DN, most pixels seemed to stay at 90 meters.

Table 3.1 NIR and TIRS 10, 11, 2 band fusion objective assessments, best findings in bold

	IHS	Brovey	PCA	Wavelet
CC	0.95071	0.9886	**0.99253**	0.99020
RMSE	51.7431	28.1597	**22.8849**	25.0625
ERGAS	5.5540	3.0226	**2.4564**	2.6902
HPCC	**0.99547**	0.69225	0.78210	0.84558

Table 3.2 Objective evaluations of NIR and OLT 2, 3, 4 band fusion, best results are in bold

	IHS	Brovey	PCA	Wavelet
CC	0.95109	0.98865	**0.99262**	0.99034
RMSE	53.0334	28.9384	**23.4059**	25.7086
ERGAS	5.6441	3.0785	**2.4897**	2.735
HPCC	**0.99709**	0.69465	0.7836	0.84876

The spectral compatibility of fused pictures was tested using the CC, the RMSE, and ERGAS. The results are shown in table 3.1 and table 3.2. As can be observed in the table above, the results of the Brovey, Wavelet, and PCA transform techniques were encouraging, however, the HIS transform technique had relatively bad results, with a lower CC and much greater RMSE and ERGAS

3.3 Image Segmentation for agriculture crop clustering

For the two high-resolution RS images, different segmentation techniques were applied as seen in Figures 3.3 and 3.4. The segmentation results were seen in vague interpretation because of various parameters. The main concern is the spatial and spectral frequency of the input image. However, the analysis of the results shows that the graph cut algorithm generates identifiable changes in land use over the period 2013 and 18 as seen in table 3.3. It displays the results of the prior segmentation methods and suggests a graph-cut approach. Each segmentation method's PRI, GCA, and VoI parameters are computed. Region-based segmentation approaches include watershed and the proposed graph technique. The quad tree approach begins at the top of the image's tree, which represents the entire image. It breaks into four small squares if it is discovered to be non-uniform (not homogenous) (the splitting process)

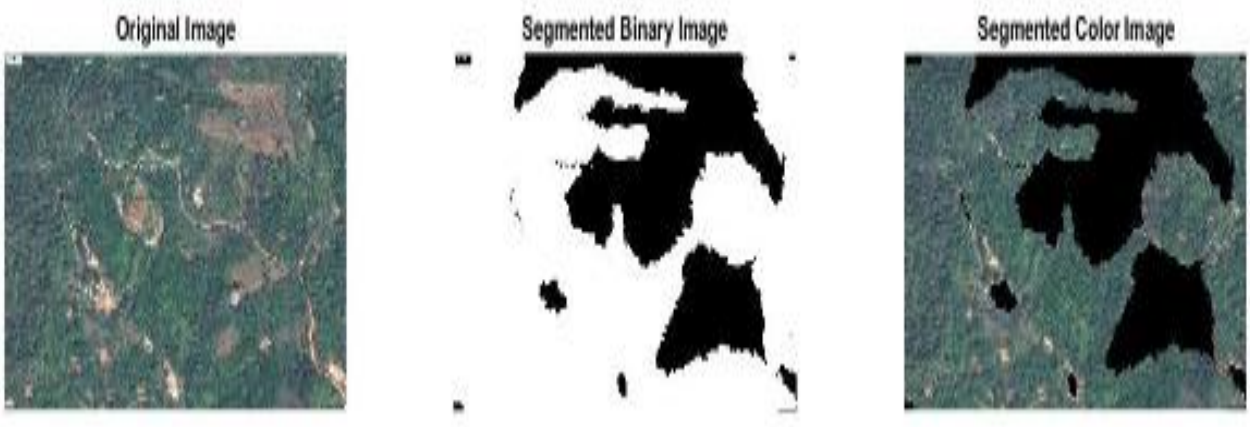

Figure 3.2: Original Image, Segmented Binary Image and Segmented Color Image

Table 3.3: Results of Segmentation Using a Region-Based Method and a Boundary-Based Method.

Segmentation Method	**PRI**	**Origin image GCE**	**Vol**	**PRI**	**Origin Image 2 GCE**	**Vol**
Watershed	0.8797	0.8778	11.8219	0.9542	0.9568	13.2924
Canny	0.2851	0.2201	5.4241	0.2030	0.1434	6.8397
Sobel	0.1543	0.0563	5.0602	0.0899	0.0427	6.6001
Graph Cut	0.8815	0.8758	12.2234	0.9572	0.9573	13.7379

For the two high-resolution RS images, figure 3.2 displays the results of the segmentation methods and suggests a graph-cut approach. The PRI, GCA, and VoI parameters are computed for each segmentation as shown in table 3.3. Region-based segmentation approaches include watershed and the proposed graph technique. The quadtree approach begins at the top of the image's tree, which represents the entire image. It breaks into four small squares if it is discovered to be non-uniform (not homogenous) (the splitting process).

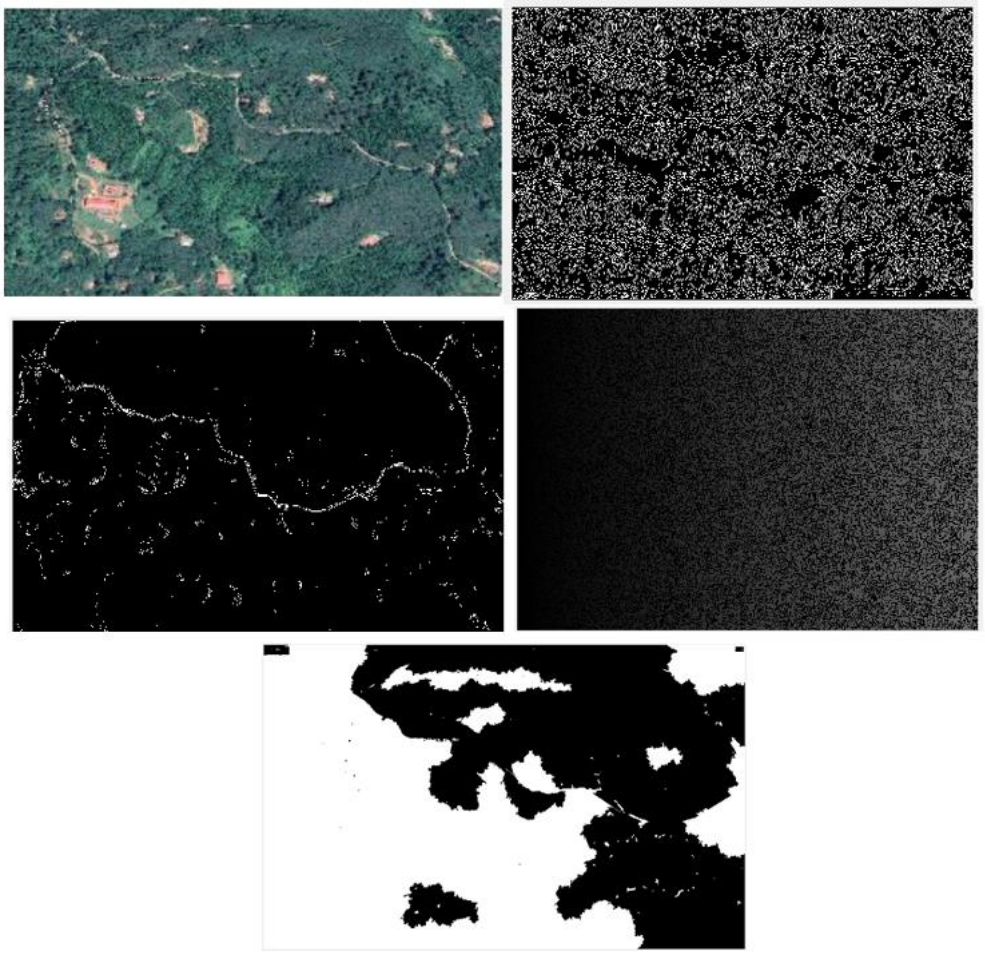

Figure 3.3: Original Image Canny Edge Detection, Sobel Edge Detection, Watershed and Graph Cut implementation on 2013 Marakanja region.

These four small squares, on the other hand, are combined as numerous connected components if they are homogeneous (the merging process). This operation is repeated until there are no more splits or merges possible. Using a pyramid or quadtree structure, the multi-resolution technique splits the image at several scales. The watershed method treats an image's gradient magnitude as a topographic surface.

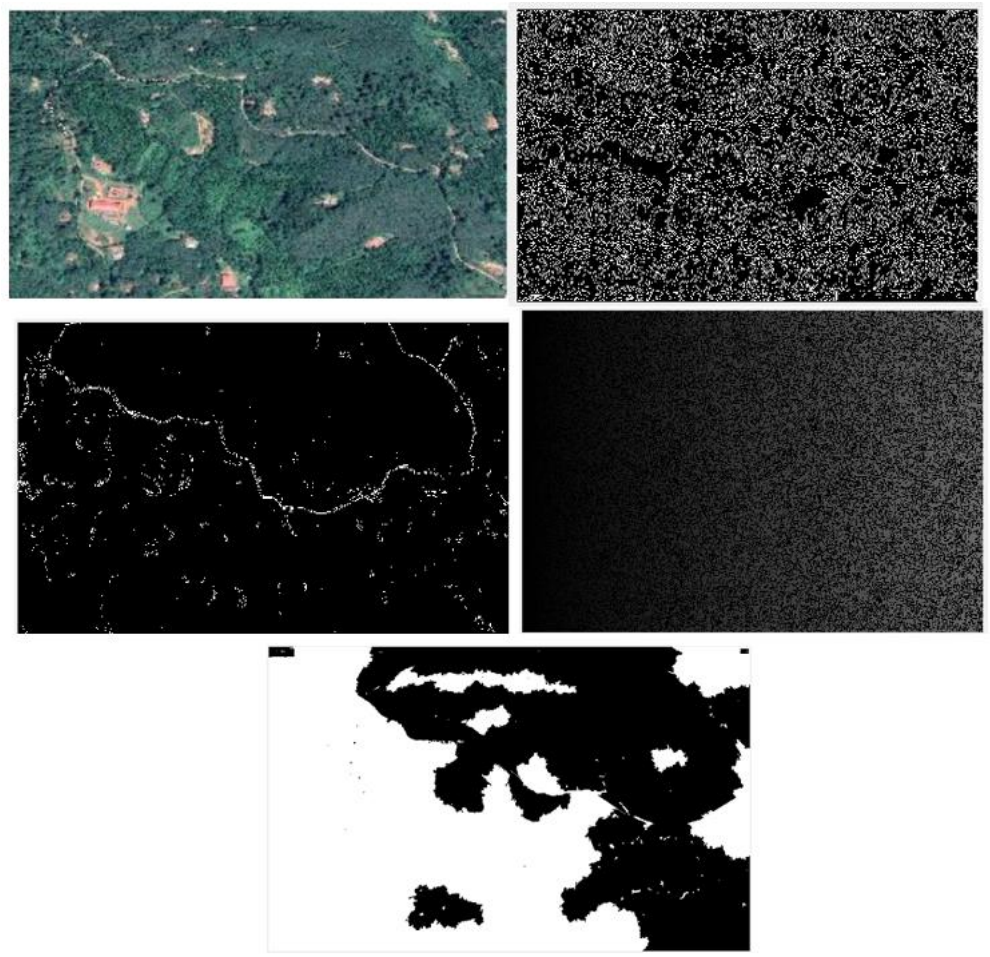

Figure 3.4: Original Image, Canny Edge Detection, Sobel Edge Detection, Watershed, and Graph Cut Implementation on 2018 Marakanja region.

Watershed lines, which represent region borders, correspond to pixels with the maximum gradient magnitude intensities. Mode discovery in an underlying probability density is revealed by a group of data samples, is characterized as the mean shift approach. Boundary-based segmentation methods include the Canny and Sobel operators.

Table 3.3 illustrates that, when the quality of the data from the assessment parameters is taken into account, the proposed graph-cut approach produces the best results. When compared to the other segmentation methods, this method's PRI value is the highest. This is because this method takes into account the spectrum, form, and texture of the image, and the segmented region is similar to the previous. As seen in Table 3.3, the results of region-based segmentation approaches outperform those of boundary-based segmentation approaches.

4. AGRICULTURE LAND CLASSIFICATION METHODS

4.1 Classification Overview

In this section, the prospects of several classification algorithms were addressed to accomplish the second objective. The competitive algorithms were used In the successive phase. The trained classification approaches were employed to create an automated system for change detection by describing diverse vegetation species and their temporal changes.

Based on spectral reflectance, image classification techniques are used to categorize the pixels in satellite data for identifying distinct earth features

such as barren land, forests, roads, settlements, water bodies, and rocks. This method is commonly used to create the LULC (Land Use Land Cover Map).

The unsupervised and supervised image classification techniques are discussed here. The remote sensing images were processed by using Qgis and Idrisi image classification tools.

A more accurate and extensively used type is supervised classification. To carry out this classification, first, collect data to select land cover classes (training sites) using a visual digitizing approach with the assistance of the user. Check to see if the software using is correctly classifying all of the satellite data.

High-resolution images will be used to acquire data on the Training site location. This is regarded as a representative of a specific type of land cover. The decision is taken based on the area covered in the class's whole range of variability.

The software helped precisely to classify the image. To identify a close match, the system determines the spectral signature of the pixels within the training region. Statistics are used to define the information, which includes the mean and variance of each class to link to all of the inputs.

Another form of classification used to classify satellite data is unsupervised classification. It's a computer-assisted classification method that's related to object-based picture categorization in certain ways. It consists of the K-means and Iso cluster algorithms It is decided on the number of classes and pixels that will be categorized according to their spectral value. The K-means clustering algorithm is used in this work under an unsupervised classification procedure.
Samples are assigned throughout each iteration based on the attribute distances between the cells in the cluster. After each iteration, the process is repeated, and each pixel is assigned to the attribute space's nearest mean.

An unsupervised classification method can be used to map satellite data for a variety of purposes, including land use and land cover mapping, among others.

4.3.2 Maximum Likelihood Classifier (MLC)
Approaches for pattern identification and remote sensing have seen an increase in investment, according to MLC [6]. It is the most used supervised classification approach and is included in practically every application for remote sensing and picture analysis. The chance that a pixel belongs to a certain class is defined by the maximum likelihood decision rule's general formulation. The Bayes rule states that classes have equal goals, and this classifier is based on it.

MLC plots LULC groups as centroids in feature space using the training-sample-based standard deviation of certain multispectral images. Likelihood curves determine the boundaries of these centroids. The likelihood degree after several that the decent sample values for each provided class are distributed normally. The Landsat pre-processed image for the classification is shown in Figure 4.4.

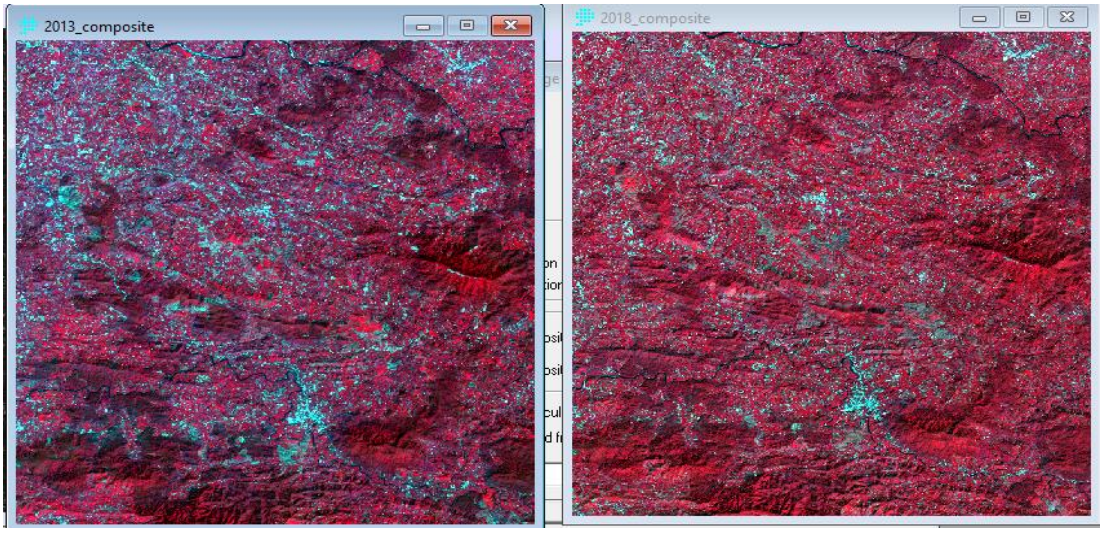

Figure 4.4: Landsat-8 images for 2013 and 2018 time duration

This demonstrates an increase in the Hughes effect. Classification accuracy climbs initially as the number of features (or measurement difficulty) rises, however, when more features are introduced, it reaches a halt and begins to dwindle. It is well accepted that data with a larger dimensionality (more measurements) has higher class spectrum reparability, but when the dimensionality is too high, it affects and reduces the accuracy of the estimation of the statistics. In some circumstances, despite the aforementioned enough training samples must be provided to give logical estimations of the mean vectors and correlation matrix to be created for each spectrum class of data, these results in inferior classification accuracy. To avoid (N) the correlation coefficient being unique in a multidimensional space, at least (N+1) observations are necessary.

4.3.2.1 Experimentation Results and Discussion

The Landsat 8 images from the years 2013 and 2018 are taken as seen in figure 4.4. The MLC classifier is applied by discriminating five major classes rubber plantation, areca, forest, and shrubs. The resultant figure 4.5 demonstrates the extent of rubber plantation which is seen in red color. It is seen that there are few acres of rubber plantation along with an equal share with the areca nut plantation.

But when we analyze the 2018 classification in figure 4.6 there is a huge change of crops. Mostly shrubs(primary forests, or cashew plantations, or banks of forests are converted into rubber plantation. From the ground truth information, there are few cases where the yellow leaf affected areca nut plantation also converted into rubber plantation

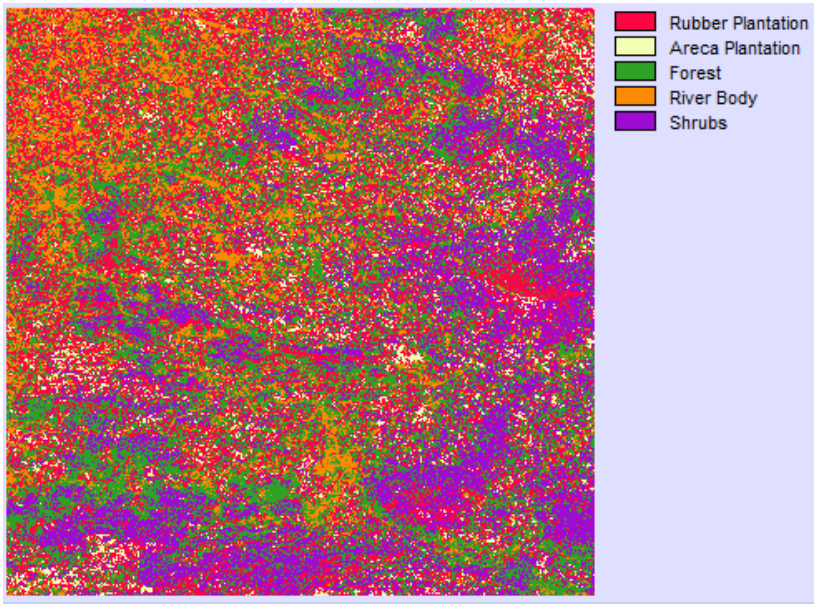

Figure 4.5: Maximum likelihood classifier 2013 results

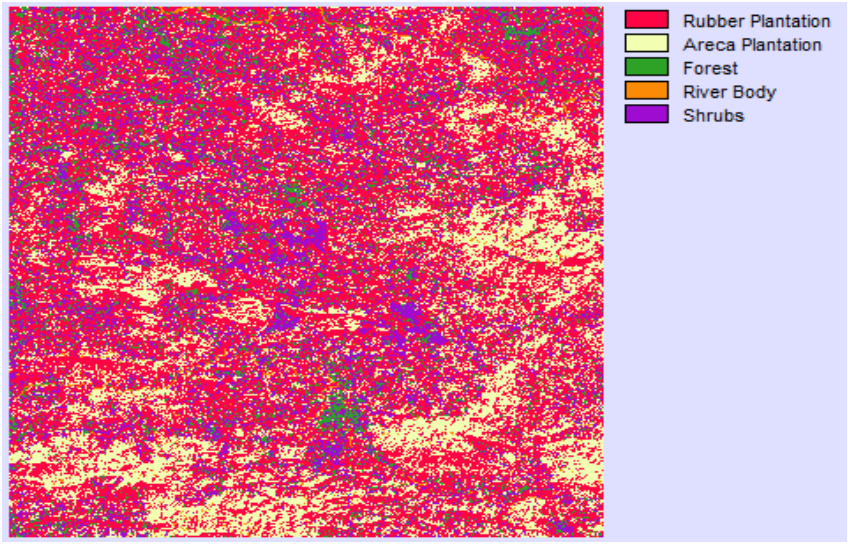

Figure 4.6 : Maximum likelihood classifier 2018 results

Despite having considerable established weaknesses in particular situations, found that the MLC obtained a better classification result as seen in table 4.1 even for data that did not have a standard distribution. To begin with, the classifier's basic assumption is violated if the image data's histogram/frequency distribution does not guarantee a normal distribution, and the results are poor or misleading. Second, the cost of classifying each pixel is an issue.

Table 4.1: Land-cover Data extracted from MLC

Reference data						
Land cover classes	**Deciduous**	**Arecanut**	**Rubber**	**Shrub**	**Row total**	**User's Accuracy in %**
Deciduous	**65**	4	22	24	115	65/115=57
Arecanut	6	**81**	5	8	100	81/100=81
Rubber	0	11	**85**	19	115	85/115=74
Shrub	4	7	3	**90**	104	90/104=87
Column total	75	103	115	141	**434**	
Producer's Accuracy (%)	65/75=87	81/103=79	85/115=74	90/141=64		
Overall Accuracy in % = (65+81+85+90)/434=74						

The square of the number of implemented feature channels increases the cost of computation. The approach works well for data with high definition and/or dimensionality, which seems to improve within-class variation; nevertheless, for data with poor image resolution and/or a small number of frequency bands. However, data with spatial precision and/or dimensional space, which seems to enhance within-class variance, performs poorly. The likelihood of class overlap in feature space increases as the amount of feature space inhabited by each class grows. Finally, the mean vector and variance-covariance matrix assessments are affected by the connection between the range of features and the sampling technique.

References

1. H. Nagendra et al., "Remote sensing for conservation monitoring: Assessing protected areas, habitat extent, habitat condition, species diversity, and threats," Ecol. Indic., vol. 33, pp. 45–59, 2013, doi: 10.1016/j.ecolind.2012.09.014.
2. F. Guttler, D. Ienco, J. Nin, M. Teisseire, and P. Poncelet, "A graph-based approach to detect spatiotemporal dynamics in satellite image time series," ISPRS J. Photogramm. Remote Sens., vol. 130, pp. 92–107, 2017, doi: 10.1016/j.isprsjprs.2017.05.013.
3. S. Li, D. Li, C. Zhang, J. Wan, and M. Xie, "RGB-D image processing algorithm for target recognition and pose estimation of visual servo system," Sensors (Switzerland), vol. 20, no. 2, 2020, doi: 10.3390/s20020430.
4. M. Vidal and J. M. Amigo, "Pre-processing of hyperspectral images. Essential steps before image analysis," Chemom. Intell. Lab. Syst., vol. 117, no. August, pp. 138–148, 2012, doi: 10.1016/j.chemolab.2012.05.009.
5. S. Ranka, R. R. Vatsavai, A. Rangarajan, M. Sethi, and Y. Yan, "Graph-based semi-supervised classification on very high resolution remote sensing images," Int. J. Big Data Intell., vol. 4, no. 2, p. 108, 2017, doi: 10.1504/ijbdi.2017.10002925.
6. V. Kumar and S. Agrawal, "Agricultural land use change analysis using remote sensing and GIS: A case study of Allahabad, India," Int. Arch. Photogramm. Remote Sens. Spat. Inf. Sci. - ISPRS Arch., vol. 42, no. 3/W6, pp. 397–402, 2019, doi: 10.5194/isprs-archives-XLII-3-W6-397-2019.
7. M. Ustuner, F. B. Sanli, S. Abdikan, M. T. Esetlili, and Y. Kurucu, "Crop type classification using vegetation indices of rapideye imagery," Int. Arch. Photogramm. Remote Sens. Spat. Inf. Sci. - ISPRS Arch., vol. 40, no. 7, pp. 195–198, 2014, doi: 10.5194/isprsarchives-XL-7-195-2014.
8. H. Blitzer, K. Stein-Ferguson, and J. Huang, "Image Processing Tools," Underst. Forensic Digit. Imaging, vol. 32, pp. 169–205, 2008, doi: 10.1016/b978-0-12-370451-1.00010-x.
9. Z. Ye, R. Dong, L. Bai, and Y. Nian, "Adaptive collaborative graph for discriminant analysis of hyperspectral imagery," Eur. J. Remote Sens.,

vol. 53, no. 1, pp. 91–103, 2020, doi: 10.1080/22797254.2020.1735947.

10. J. B. Fasquel and N. Delanoue, "A graph based image interpretation method using a priori qualitative inclusion and photometric relationships," IEEE Trans. Pattern Anal. Mach. Intell., vol. 41, no. 5, pp. 1043–1055, 2019, doi: 10.1109/TPAMI.2018.2827939.
11. I. Pre-processing, "Image Pre-Processing," pp. 1–7.
12. K. Ennouri, A. Kallel, and R. Albano, "Remote sensing: An advanced technique for crop condition assessment," Math. Probl. Eng., vol. 2019, 2019, doi: 10.1155/2019/9404565.
13. J. Shepherd, P. Bunting, and J. Dymond, "Operational Large-Scale Segmentation of Imagery Based on Iterative Elimination," Remote Sens., vol. 11, no. 6, p. 658, 2019, doi: 10.3390/rs11060658.
14. S. SankarNath and P. Rakshit, "A Survey of Image Processing Techniques for Emphysema Detection," Int. J. Comput. Appl., vol. 114, no. 15, pp. 7–13, 2015, doi: 10.5120/20052-1983.
15. F. Guttler, D. Ienco, J. Nin, M. Teisseire, and P. Poncelet, "A graph-based approach to detect spatiotemporal dynamics in satellite image time series," ISPRS J. Photogramm. Remote Sens., vol. 130, pp. 92–107, 2017, doi: 10.1016/j.isprsjprs.2017.05.013.
16. A. Sanfeliu, R. Alquézar, J. Andrade, J. Climent, F. Serratosa, and J. Vergés, "Graph-based representations and techniques for image processing and image analysis," Pattern Recognit., vol. 35, no. 3, pp. 639–650, 2002, doi: 10.1016/S0031-3203(01)00066-8.
17. L. Hu, C. Qi, and Q. Wang, "Spectral-Spatial Hyperspectral Image Classification Based on Mathematical Morphology Post-Processing," Procedia Comput. Sci., vol. 129, pp. 93–97, 2018, doi: 10.1016/j.procs.2018.03.054.
18. D. Pulido, J. Salas, M. Rös, K. Puettmann, and S. Karaman, "Assessment of Tree Detection Methods in Multispectral Aerial Images," pp. 1–22, 2020, doi: 10.3390/rs12152379.
19. J. C. Tilton, S. Aksoy, and Y. Tarabalka, "Image segmentation algorithms for land categorization," Remote. Sensed Data Charact. Classif. Accuracies, vol. 1, no. September, pp. 317–342, 2015, doi: 10.1201/b19294.
20. K. Amiri, M. Farah, and U. M. Leloglu, "BoVSG: bag of visual SubGraphs for remote sensing scene classification," Int. J. Remote Sens., vol. 41, no. 5, pp. 1986–2003, 2020, doi: 10.1080/01431161.2019.1681602.
21. Y. Wang et al., "A Three-Layered Graph-Based Learning Approach for Remote Sensing Image Retrieval," IEEE Trans. Geosci. Remote Sens., vol. 54, no. 10, pp. 6020–6034, 2016, doi: 10.1109/TGRS.2016.2579648.
22. S. S. Sawant and M. Prabukumar, "A review on graph-based semi-supervised learning methods for hyperspectral image classification," Egypt. J. Remote Sens. Sp. Sci., no. xxxx, pp. 1–6, 2018, doi: 10.1016/j.ejrs.2018.11.001.
23. Y. Song and J. Qu, "Real-time segmentation of remote sensing images with a combination of clustering and Bayesian approaches," J. Real-Time Image Process., no. 0123456789, 2020, doi: 10.1007/s11554-020-00990-z.
24. Y. Shao, J. Ren, and J. B. Campbell, Multitemporal remote sensing data analysis for agricultural application, vol. 1–9. Elsevier, 2017.
25. J. B. Fasquel and N. Delanoue, "A graph based image interpretation method using a priori qualitative inclusion and photometric relationships," IEEE Trans. Pattern Anal. Mach. Intell., vol. 41, no. 5, pp. 1043–1055, 2019, doi: 10.1109/TPAMI.2018.2827939.
26. C. S. Reddy, C. S. Jha, and V. K. Dadhwal, "Assessment and monitoring of long-term forest cover changes (1920-2013) in Western Ghats biodiversity hotspot," J. Earth Syst. Sci., vol. 125, no. 1, pp. 103–114, 2016, doi: 10.1007/s12040-015-0645-y.
27. T. V. Ramachandra and S. Bharath, "Carbon Sequestration Potential of the Forest Ecosystems in the Western Ghats, a Global Biodiversity Hotspot," Nat. Resour. Res., vol. 29, no. 4, pp. 2753–2771, 2020, doi: 10.1007/s11053-019-09588-0.
28. S. Osher, "PRE-PROCESSING AND CLASSIFICATION OF HYPERSPECTRAL IMAGERY VIA SELECTIVE INPAINTING Victoria Chayes Rasika Bhalerao California Research Training Program in Computational and Applied Mathematics University of California , Los Angeles , Department of Mathem," IEEE Int. Conf. Acoust. Speech, Signal Process. 2017, pp. 6195–6199, 2017.
29. R. P. Sishodia, R. L. Ray, and S. K. Singh, "Applications of remote sensing in precision agriculture: A review," Remote Sens., vol. 12, no. 19, pp. 1–31, 2020, doi: 10.3390/rs12193136.
30. P. Lemenkova, "Using K-means algorithm classifier for urban landscapes classification in Taipei area , Taiwan Polina Lemenkova To cite

this version : HAL Id : hal-02425701," 2019.

31. I. S. Sitanggang and H. Harianja, "K-means clustering visualization on agriculture potential data for villages in bogor using mapserver," no. August, pp. 5–6, 2008.
32. N. L. Distillation, "Noisy Label Distillation," pp. 1–21, 2020, doi: 10.3390/rs12152376.
33. R. Neware and P. A. Khan, "Identification of agriculture areas in satellite images using Supervised Classification Technique," no. April, 2018.
34. Y. Xie, Z. Sha, and M. Yu, "Remote sensing imagery in vegetation mapping: a review," J. Plant Ecol., vol. 1, no. 1, pp. 9–23, 2008, doi: 10.1093/jpe/rtm005.
35. P. Mhangara, W. Mapurisa, and N. Mudau, "Comparison of image fusion techniques using Satellite pour l'Observation de la terre (SPOT) 6 satellite imagery," Appl. Sci., vol. 10, no. 5, pp. 1–13, 2020, doi: 10.3390/app10051881.
36. X. Wang, "Graph based approaches for image segmentation and object tracking To cite this version," Ec. Cent. Lyon, 2015.